# EVALUATION OF BIOLOGICAL FILMS TO SEA SURFACE ROUGHNESS OBSERVED BY SAR

D. Hasegawa [a,*], I. Asanuma [a], Y. Arvelyna [a]

[a] Tokyo University of Information Sciences, 4-1, Onaridai, Wakaba, Chiba, Japan  -
(e08012dh, asanuma, yessy_a)@edu.tuis.ac.jp

**Commission VIII, WG VIII/6**

**KEY WORDS:**  SAR, Ocean color, Surface wind, Surface roughness, Biological activity

**ABSTRACT:**

The images of the sea surface roughness observed by PALSAR on ALOS over the Philippine Archipelagos were studied with other opportunities of satellite observations including MODIS and other measurement to understand an imaging mechanism by SAR.  The Tabulas Strait and the Mindanao Sea, which are connecting the Pacific and the South China Sea and blocking the North Equatorial Current, were selected to study the physical and biological contribution to the sea surface roughness observed by SAR.  The data from MODIS on TERRA and AQUA were refereed as a semi-synchronized observation and the reanalysis wind data from NCEP were refereed as the observation on the same day.  The intensity of sea surface roughness is represented as the power spectrum in the frequency domain from each specific region, where the roughness is modulated by the wind, the upwelling, the rain, and the surface film associated with biological activities.  Although the chlorophyll-a concentration observed by MODIS is not the direct estimate of the surface film, the chlorophyll-a concentration would be refereed to represent the surface film as the zooplankton being expected proportional to chlorophyll-a concentration and the associated products as a result of the surface film being expected proportional. The wind direction and speed from the NCEP data set were applied to analyze the contribution to the sea surface roughness, which has a positive contribution against the surface film. The power spectrum obtained from the different texture patterns in the sea surface roughness observed by SAR exhibited the different intensities in the frequency domain.  The correlation plots between the power spectrum at the certain frequency and the chlorophyll-a concentration showed a good relationship, where the negative correlation was observed as the increase of chlorophyll-a concentration.  The reduction of surface roughness by the surface film associated with the biological activities were confirmed under a limited a wind speed .

## 1.  INTRODUCTION

A contribution of biological effect to the sea surface roughness observed by SAR has been discussed since the operation of SAR on SEASAT.  In the first stage of SAR interpretation, various properties of the ocean surface were studied and the imaging mechanism of the ocean surface was discussed (Thomson et al., 1981, Stewart, 1985, Gotwols and Thompson, 1994). In the second stage, SAR data were interpreted from physical properties with other sensors.  Nilsson and Tildesley (1995) suggested that changes in boundary layer stability due to changing sea surface temperature do not appear to be a principal cause of imaging of meso-scale features through the analysis with a simultaneous observation between SAR and the Advanced Very High Resolution Radiometer (AVHRR). Johannessen et al. (1996) studied a cross correlation between the surface roughness pattern imaged by SAR and the sea surface temperature distribution imaged by AVHRR.  The backscatter variations by natural surface films were suggested to be the most likely explanation for the imaging mechanism from the Coastal Zone Color Scanner (CZCS) in the past (Nilsson and Tildesley, 1995). A possible contribution of ocean color sensors was suggested to explore the mechanism of damping by the natural films due to the increased biological productivity (Johannessen et al., 1996).  In the third stage, contributions of biological activities to SAR imaging mechanism were studied.  Moore and Marra (2002) observed and analyzed the variability in the bloom events in the Strait of Ombai with the Sea-viewing Wide Field-of-view Sensor (SeaWiFS), AVHRR, and SAR.  Asanuma et al. (2003)

analyzed a damping of surface roughness by the phytoplankton associated with upwelling and associated higher primary productivity through a simultaneous observation with SAR and SeaWiFS.  Lin et al. (2002) analyzed the variation of radar cross sections relative to the chlorophyll-a concentration with a simultaneous observation between ERS-2 SAR and SeaWiFS and made a quantification of radar cross section and chlorophyll-a concentration.  Johannessen et al. (2005) proposed one radar imaging mechanism with the normalized radar cross section.  The imaging mechanism of sea surface roughness observed by SAR is getting clear but it is still under study because of the complexities of phenomena including biological activities with other physical contributions like wind, upwelling, currents, internal waves, and so on such as the large scale wave and small scale ones which are sensitive as the radar scattering surface.
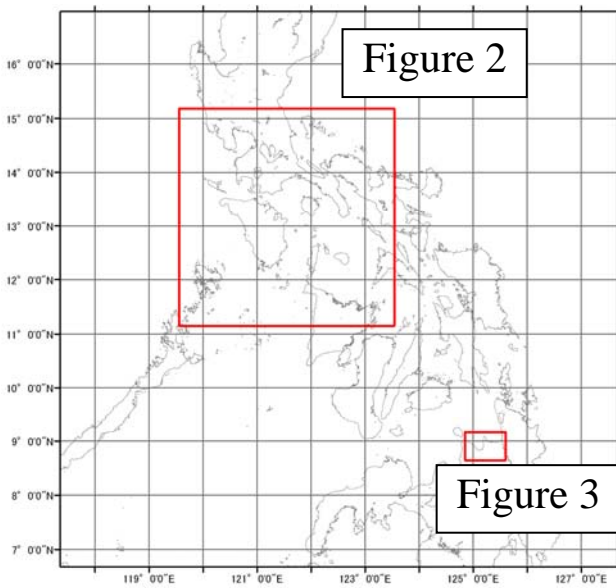
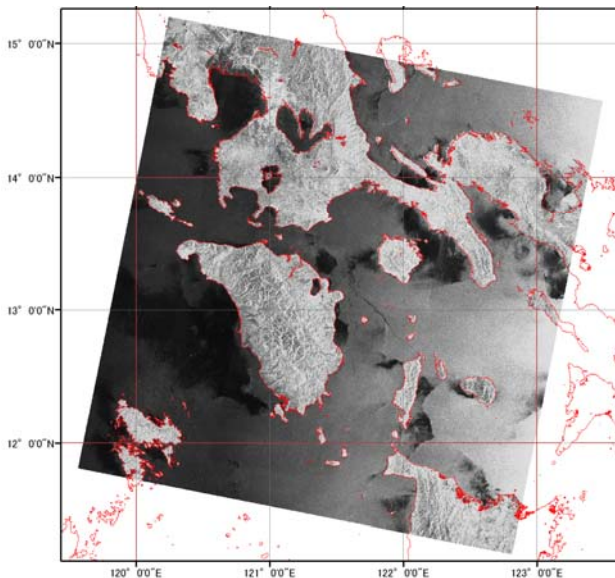Figure 1. Location of SAR observation over Philippine.



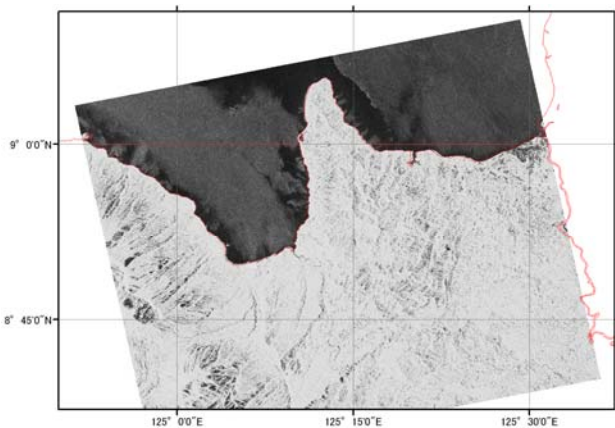Figure 2. Wide Scan SAR image by PALSAR on June 14, 2007.



Figure 3. Image observed by PALSAR on June 28, 2007.

The region in this study is the Philippine Archipelagos. In this region, the low-latitude western boundary circulation in the far western equatorial Pacific Ocean affects currents, running into the Philippine Sea or running southward along the Philippine Archipelagos (Lukas et al., 1991). The intrusion of the Philippine Sea Water into the South China Sea exhibits a seasonal variation (Shaw, 1991). The water mass in the Philippine Sea has an important element in the interaction between El Nino-Southern Oscillation (ENSO) and the East Asia Monsoon (Watanabe and Jin, 2002; Zhou and Yu, 2005; Yang et al., 2007). In the initial study, the Mindanao Sea was selected to interpret the surface roughness observed by SAR and biological activities. Winds are a major contribution to determine the surface roughness in this region, and the seasonally reversing monsoon winds also play an important role in determining the upper ocean circulation (Metzger and Hurlburt, 1996).

The surface phenomena observed by PALSAR on ALOS were analyzed in the power spectrum domain relative to chlorophyll-a concentration, which may have a significant correlation with zoo plankton, to discuss a contribution of biological film in the surface to reduce the surface roughness. And the surface wind, reproduced by NCEP, was referred to discuss its threshold to mask the biological contribution to the surface roughness.

## 2. MATERIALS AND METHOD

### 2.1 PALSAR

The Advanced Land Observing Satellite (ALOS) was launched on January 24, 2006 by the Japan Aerospace Exploration Agency (JAXA). The Phased Array type L-band Synthetic Aperture Radar (PALSAR) is an active microwave sensor on ALOS using L-band frequency to achieve cloud-free and day-and-night observation (JAXA, 2008). PALSAR is selectively operated in a conventional fine resolution mode and in an advantageous observation mode as listed on Table 1. In this study, one image is taken by a ScanSAR mode with the swath of 350 km and the spatial resolution of 100 m, and other image is taken by a fine mode with the swath of 40 km and the spatial resolution of 7 m.

| Mode | Fine | | ScanSAR |
|---|---|---|---|
| Center Frequency | 1270 MHz (L-band) | | |
| Chirp bandwidth | 28 MHZ | 14 MHz | 14 MHz 28MHz |
| Polarization | HH or VV | HH+HV or VV+VH | HH or VV |
| Incident | 8 to60 deg. | 8 to 60 deg. | 18 to 43 deg. |
| Range resolution | 7 to 44 m | 14 to 88 m | 100m (multibok) |
| Observation swath | 40 to 70 km | 40 to 70 km | 250 to 350 km |

Table 1. PALSAR specification

### 2.2 Chlorophyll-a concentration observed by MODIS

The distribution of chlorophyll-a concentration and sea surface temperature are mapped from the Moderate Image Scanning Radiometer (MODIS) dataset, which is available at the ocean color web site (http://oceancolor.gsfc.nasa.gov). The semi-
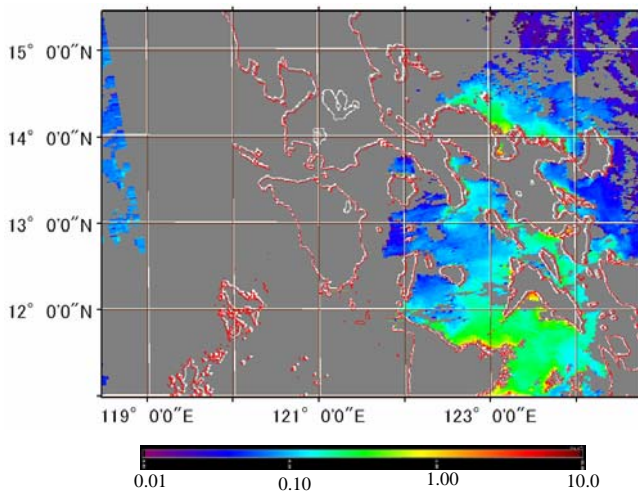
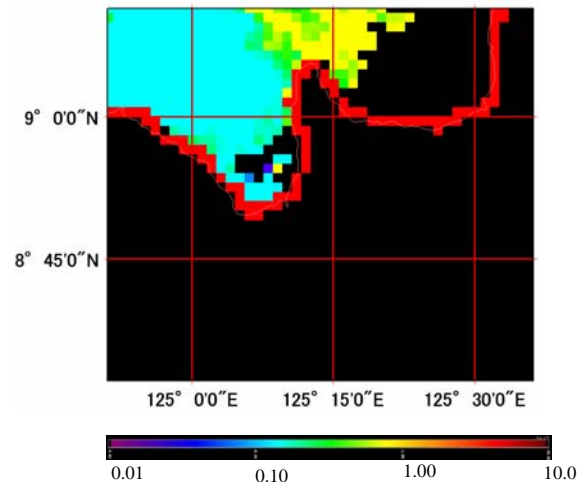Figure 4. Chlorophyll-a distribution observed by MODIS on June 14, 2007 in mg m$^{-3}$.



Figure 6. Chlorophyll-a distribution observed by MODIS on June 28, 2007 in mg m-3.
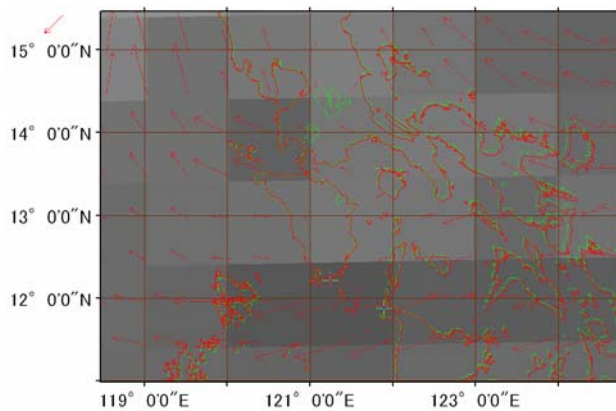


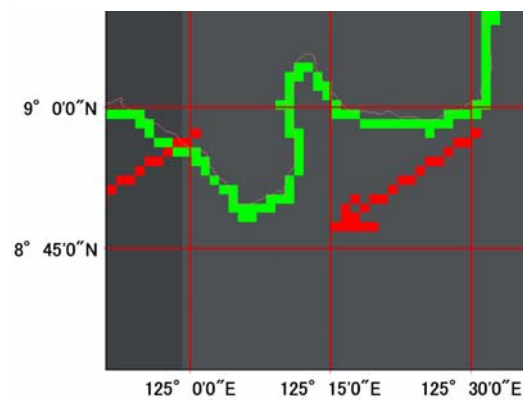Figure 5. Surface wind vectors on June 14, 2007, reproduced by NCEP.



Figure 7. Surface wind vectors on June 28, 2007, reproduced by NCEP.

simulcast observations by MODIS synchronized to the SAR without clouds were down loaded in the level-2 format and were mapped on the region of interest with the SeaWiFS Data Analysis System (SeaDAS).

## 2.3 Surface wind analysis by NCEP

Surface wind data were applied for this study from the data set opened by the ocean color group at the Goddard Space Flight Center of NASA. The ancillary data set including NCEP Meteorological (MET) and TOMS/TOVS Ozone (OZ) is necessary to process SeaWiFS or MODIS data (NASA, 2008).

## 2.4 Texture analysis in the frequency domain

In this study, the texture of the sea surface roughness is analyzed in the frequency domain. Although a directional component of the sea surface roughness is missing, one line digital data was sampled from SAR image including the roughest and smoothest locations manually. Digital data from one line is put into the Excel sheet so as to get the power spectrum as a sum of square of real and imaginary part using the First Fourier Transform (FFT). The largest phenomenon is the swell and its spectrum power is given at the lowest frequency. The smallest phenomenon is the breaking wave and/or the capillary one and its spectrum power is given at the highest frequency. The natural films will damp the surface roughness and its contribution could be observed at higher

frequency. As we have a different special resolution between the fine SAR and the scan SAR image, a same spatial distance was selected and its frequency was selected to get its power spectrum.

## 3. RESULTS AND DISCUSSION

### 3.1 Satellite data

Figure 1 shows the locations of two SAR data on the Philippine Archipelagoes.

Figure 2 shows the ScanSAR image of the Tablus Straight connecting between the Sibyan Sea and the Sulu Sea taken on June 14, 2007. A rough surface is widely scattered in this region with some calm water behind islands. According to the surface wind, Figure 5, provided by NCEP, the East wind was dominant in the Sibyan Sea and in the Sulu Sea, and the East-East-South wind was dominant in the Pacific and in the South China Sea. These East and East-South-East winds generated the rough surface observed in the PALSAR image. Chlorophyll-a concentration in the Tablus Straight was less than 0.1 mg m$^{-3}$, and a slightly higher concentration around 0.5 mg m$^{-3}$ was observed in the Visayan Sea and around the Calagua Islands (Figure 4).

Figure 3 shows the Fine SAR image of water off the Diuata Peninshula located at the northern part of the Mindanao Island. In the East side and the North-west side of the Diuata Peninshula, a  and the North-west  According to Figure 6 of chlorophyll-a distribution, a high chlorophyll-a water was observed on the North-east region of the Diuata Peninshula. Figure 7 shows a North-east wind of 4.4 m s-1 was blowing to the coast.  The Eckman pumping is expected to the North-west ward by the dominant North-east wind with entrainments of nutrients to the surface layer and promoting a primary production.

### 3.2 Power spectrum and relationship to chlorophyll-a concentration and wind speed

Figure 8, 9 and 10 show the cross scatter diagram between the power spectrum and wind speed or chlorophyll-a concentration. On June 14, 2007, a group of lower power spectrum was observed at locations, where low wind speed less than 3.0 m s$^{-1}$ was observed.  In contrast, a group of high power spectrum was observed at locations, where high wind speed of 5.0 m s-1 was observed.  These two groups of power spectrum indicate that the surface roughness is enhanced by the surface wind.

Figure 9 shows a scatter plot between the power spectrum and the chlorophyll-a concentration observed on June 14, 2007. The associated number for each point is indicating the same number as on Figure 8.  It is possible to group the locations of 1, 5, 7, and 8 as a high power spectrum and a big variation of chlorophyll-a concentration, because of high wind speed as grouped on Figure 8.  In contrast, the locations 2, 4, 3, and 6 exhibited lower power spectrum. It is supposed that the stations in higher chlorophyll-a concentration will exhibit lower power spectrum by our hypothesis, where the biological film from zooplankton may increase concurrently with an increase of chlorophyll-a concentration with reducing the surface roughness.  But the locations 6, 4, and 2 exhibited the decrease of surface roughness as a function of chlorophyll-a concentration.   The location 3 is difficult to explain in this concept why the location 3 exhibited a high power spectrum with a low wind speed and a high chlorophyll-a concentration.

Figure 10 is a scatter plot between the power spectrum and the chlorophyll-a concentration on June 28, 2007.  It was difficult to make a scatter plot between the power spectrum and the wind speed, because of the location is very limited to the coastal region and the difference of wind speed was not observed in this region.
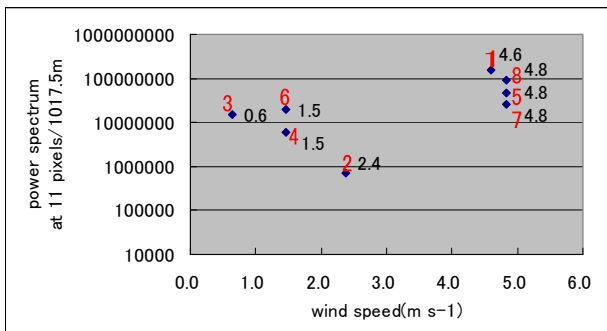


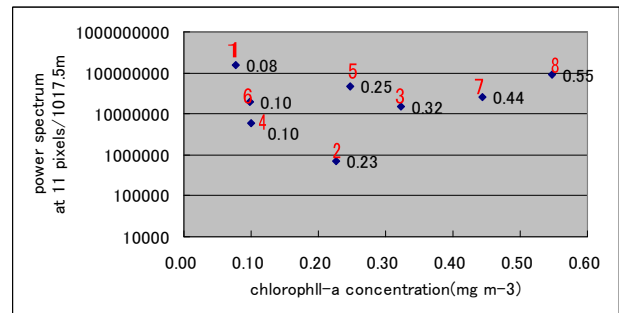Figure 8.  Scatter plot between wind speed and power spectrum on June 14, 2007.



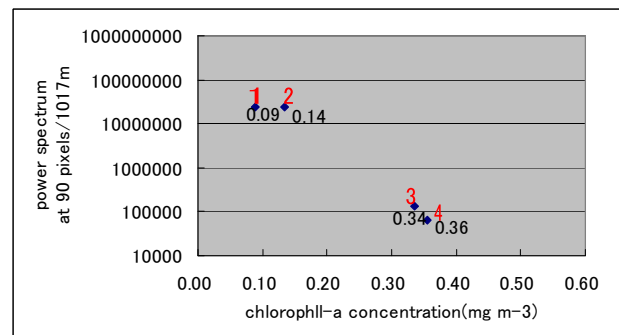Figure 9.  Scatter plot between chlorophyll-a concentration and power spectrum on June 14, 2007.



Figure 10.  Scatter plot between wind speed and power spectrum on June 28, 2007.

### 4.  SUMMARY

The observations of surface roughness by the PALSAR on ALOS on the Philippine Archipelago were examined to find a relationship among a surface roughness, a negative component of biological film, and a positive component of surface wind, with the semi-simulcast observations by the MODIS and with the NCEP wind speed data. The sea surface roughness in this region exhibited a various intensity of backscatters, but the large wave patterns such as swells or currents were not observed because of archipelagos, which are suppressing the direct entrance of currents or swells from the open water.

The observation period by the SAR in this study was in June, while is the South-east wind was dominant.  The open water, which can gain a sufficient wind blowing distance, was observed as bright patterns.  Some regions close to islands was observed as dark patterns, because of lower wind speed. Against these general interceptions, we have studied a possibility of biological films to reduce a surface roughness with an assumption that the biological film has a significant correlation with a population of zooplankton and zooplankton has one to one relationship with phytoplankton.  A positive component to surface roughness by a surface wind could be given from NCEP observation.   A negative component to surface roughness by a biological file could be indirectly estimated from chlorophyll-a concentration from MODIS observation.

In the previous studies, films damping surface roughness are explained as the chemical substances such as protein, lipids, saccharoids, organic acids and metals associated with the

organic matter (Espedal et al., 1996 and 1998). Line et al. (2002) proposed the relationship between the normalized radar cross section and the chlorophyll-a concentration with the low wind condition. As demonstrated in this study, the actual ocean has the various combination of parameters such as the natural film damping, the surface wind, and the physical signature of surface. For this difficulty of radar imaging model, various models were proposed in the normalized radar cross section (Johannessen et al., 2005).

In this paper, a possibility to describe the radar imaging in the spectrum domain was discussed, which is observed as the difference of texture on the sea surface.

## REFERENCES

Asanuma, I., K. Matsumoto, H. Okano, T. Kawano, N. Hendiarti, and S. I. Sachoemar, 2003. Spatial distribution of phytoplankton along the Sunda Islands: Them monsoon anomaly in 1998, *J. Geophys. Res.*, 108, C6(3202), doi:10.1029/1999JC000123.

Espedal, H. A., O. M. Johannessen, J. A. Johannessen, E. Dano, D. R. Lyzenga, and J. C. Knulst, 1998. COASTWATCH'95: ERS 1/2 SAR detection of natural film on the ocean surface, *J. Geophys. Res.*, 103, C11, 24,969-24,982.

Espedal, H. A. and O. M. Johannessen, 1996. Satellite detection of natural films on the ocean surface, *Geophys. Res. Letter.*, 23, 22, 3151-3154.

Gotwols, B. L., and D. R. Thompson, 1994. Ocean microwave backscatter distributions, *J. Geophys. Res.*, 99, 9741-9750.

JAXA, 2008. Phased Array type L-band Synthetic Aperture Radar, http://www.eorc.jaxa.jp/ALOS/about/palsar.htm (accessed April 29, 2008).

Johannessen, J. A., R. A. Shuchman, G. Digranes, D. R. Lyzenga, C. Wackerman, O. M. Johannessen, and P. W. Vachon, 1996. Coastal ocean fronts and eddies imaged with ERS 1 synthetic aperture radar, *J. Geophys. Res.*, 101, C3, 6651-6667.

Johannessen, J. A., V. Kudryavtsev, D. Akimov, T. Eldevik, N. Winther, and B. Chapron, 2005. On radar imaging of current features: 2. Mesoscale eddy and current front detection, *J. Geophys. Res.*, 110, C07017, doi:10.1029/2004JC002802.

Lin, I., L. Wen, K. Liu, W. Tsai, and A. K. Liu, 2002. Evidence and quantification of the correlation between radar backscatter and ocean colour supported by simultaneously acquired in situ sea truth, *Geophys. Res. Lett.*, 29(10), 10.1029/2001GL014039.

Lukas, R., E. Firing, P. Hacker, P. L. Richardson, C. A. Collins, R. Fine, and R. Gammon, 1991. Observations of the Mindanao current during the Western Equatorial Pacific Ocean Circulation Study, *J. Geophys. Res.*, 96 (C4), 7089-7104.

Metzger, E. J. and H. E. Hurlburt, 1996. Coupled dynamics of the South China Sea, the Sulu Sea, and the Pacific Ocean, *J. Geophys. Res.*, 101(C5), 12,331-12,352.

Moore II, T. S., and J. Marra, 2002. Satellite Observations of bloom events in the Strait of Ombai: Relationships to monsooms and ENSO, *Geochem. Geophys. Geosys.*, 3, 2. 1017, doi:10.1029/2001GC000174.

NASA, 2008. Ancillary Products for Ocean Color, http://oceancolor.gsfc.nasa.gov/ftp.html.

Nilsson, C. S., and P. C. Tildesley, 1995. Imaging of oceanic features by ERS 1 synthetic aperture radar, *J. Geophys. Res.*, 100, C1, 953-967.

Shaw, P. –T., 1991. The seasonal variation of the intrusion of the Philippine Sea Water into the South China Sea, *J. Geophys. Res.*, 96(C1), 821-827.

Stewart, R. H., 1995. *Methods of Satellite Oceanography*, 360 pp., University of California Press, Berkeley.

Tompson, T. W., D. E. Weissman, and F. I. Gonzalez, 1981. Seasat Sar Cross-Section Modulation by Surface Winds: Goasex Observations, *Geophys. Res. Lett.*, 8(2), 159-162.

Watanabe, M. and F. Jin, 2002. Role of Indian Ocean warming in the development of Philippine Sea anticyclone during ENSO, *Geophs. Res. Lett.*, 29(10), 10.1029/2001GL014318.

Yang, J., Q. Liu, S. Xie, Z. Liu, and L. Wu, 2007. Impact of the Indian Ocean SST basin mode on the Asian summer monsoon, *Geophys. Res. Lett.*, 34(L02708), doi:10.1029/2006GL028571.

Zhou, T. and R. Yu, 2005. Atmospheric water vapor transport associated with typical anomalous summer rainfall patterns in China, *J. Geophys. Res.*, 110(D08104), doi:10.1029/ 2004JD005413.